

Received:
3 November 2014

Revised:
28 January 2015

Accepted:
2 February 2015

doi: 10.1259/bjr.20140728

Cite this article as:

Arcangeli S, Agolli L, Portalone L, Migliorino MR, Lopergolo MG, Monaco A, et al. Patterns of CT lung injury and toxicity after stereotactic radiotherapy delivered with helical tomotherapy in early stage medically inoperable NSCLC. *Br J Radiol* 2015;88:20140728.

FULL PAPER

Patterns of CT lung injury and toxicity after stereotactic radiotherapy delivered with helical tomotherapy in early stage medically inoperable NSCLC

¹S ARCANGELI, MD, ²L AGOLLI, MD, ³L PORTALONE, MD, ⁴M R MIGLIORINO, MD, ⁵M G LOPERGOLO, MD, ¹A MONACO, MD, ¹J DOGNINI, MD, ⁶M C PRESSELLO, MSc, ²S BRACCI, MD and ¹V DONATO, MD

¹Department of Radiotherapy, Azienda Ospedaliera San Camillo-Forlanini, Rome, Italy

²Department of Radiotherapy, Sant' Andrea Hospital, University of Rome, Rome, Italy

³Department of Thoracic Oncology, 2nd Pulmonary Oncological Unit, Azienda Ospedaliera San Camillo-Forlanini, Rome, Italy

⁴Department of Thoracic Oncology, 1st Pulmonary Oncological Unit, Azienda Ospedaliera San Camillo-Forlanini, Rome, Italy

⁵Department of Thoracic Surgery, Azienda Ospedaliera San Camillo-Forlanini, Rome, Italy

⁶Department of Medical Physics, Azienda Ospedaliera San Camillo-Forlanini, Rome, Italy

Address correspondence to: Dr Stefano Arcangeli

E-mail: stefano.arcangeli@yahoo.it

Objective: To evaluate toxicity and patterns of radiologic lung injury on CT images after hypofractionated image-guided stereotactic body radiotherapy (SBRT) delivered with helical tomotherapy (HT) in medically early stage inoperable non-small-cell lung cancer (NSCLC).

Methods: 28 elderly patients (31 lesions) with compromised pulmonary reserve were deemed inoperable and enrolled to undergo SBRT. Patterns of lung injury based on CT appearance were assessed at baseline and during follow up. Acute (6 months or less) and late (more than 6 months) events were classified as radiation pneumonitis and radiation fibrosis (RF), respectively.

Results: After a median follow-up of 12 months (range, 4–20 months), 31 and 25 lesions were examined for acute and late injuries, respectively. Among the former group, 25 (80.6%) patients showed no radiological changes. The CT appearance of RF revealed modified conventional, mass-like and scar-like patterns in three, four and three

lesions, respectively. No evidence of late lung injury was demonstrated in 15 lesions. Five patients developed clinical pneumonitis (four patients, grade 2 and one patient, grade 3, respectively), and none of whom had CT findings at 3 months post-treatment. No instance of symptomatic RF was detected. The tumour response rate was 84% (complete response + partial response). Local control was 83% at 1 year.

Conclusion: Our findings show that HT-SBRT can be considered an effective treatment with a mild toxicity profile in medically inoperable patients with early stage NSCLC. No specific pattern of lung injury was demonstrated.

Advances in knowledge: Our study is among the few showing that HT-SBRT represents a safe and effective option in patients with early stage medically inoperable NSCLC, and that it is not associated with a specific pattern of lung injury.

Surgery is the standard treatment for early stage non-small-cell lung cancer (NSCLC), with an overall survival of about 50–70% in Stage I patients.¹ In clinical practice, however, patients with lung tumours, primary or metastatic, often present with related symptoms, advanced age and associated comorbid conditions. Unfortunately, most of them are excluded from clinical trials that are designed to inform practice, creating major evidence gaps. This clinical scenario is expected to further increase the number of cases in the elderly,^{2,3} with the consequence that, if untreated, the survival rates of these patients can be severely poor.⁴ Tackling this population represents a therapeutic challenge, and new opportunities exist to improve the management

and outcomes for elderly people with coexisting illnesses. In previous years, there has been much evidence of good outcomes obtained with stereotactic body radiotherapy (SBRT) for primary tumours or metastases in the lung for inoperable patients,^{5–8} and the introduction of SBRT has improved population-based survival in Stage I NSCLC.^{9,10}

Among the various treatment delivery units, helical tomotherapy (HT) is a kind of image-guided system that is able to deliver intensity-modulated radiation therapy (IMRT) by combining a continuously rotating fan beam with synchronous couch movement.^{11,12} While dosimetric

findings have shown that such capabilities can potentially translate into the delivery of an increased tumour dose with doses to normal tissues decreased compared with other techniques,^{13,14} only a limited number of patients were included in recent studies that have addressed the feasibility of hypofractionated or ablative RT regimens for lung tumours treated with HT.^{15–21} The helical radiation delivery method is associated with low-dose spread¹² to the normal lung and can potentially result in patterns of lung injury that might be different than those observed with conventional three-dimensional conformal RT (3D-CRT) or other SBRT techniques. These latter issues raise some concerns, especially in elderly patients, with frailties or comorbidities, given the risk that the potential benefits of SBRT might be hampered by an increased risk of toxicity that can be life threatening or at least substantially compromise their quality of life.

The aim of the present study is to evaluate treatment-related toxicity and patterns of radiologic lung injury on CT images after image-guided SBRT delivered with HT (HT-SBRT) for patients with early stage medically inoperable NSCLC.

METHODS AND MATERIALS

Patients' characteristics

28 patients with early stage NSCLC were deemed inoperable from our thoracic oncology tumour board owing to advanced age and/or a compromised pulmonary reserve and were enrolled to undergo SBRT. Patients had to adhere to the following characteristics: maximum tumour diameter <50 mm; advanced age (75 years or more) and/or a diagnosis of severe chronic obstructive pulmonary disease (COPD), categorized according to the Global Initiative for Obstructive Lung Disease (GOLD) guidelines;²² life expectancy of more than 6 months; performance status (Eastern Cooperative Oncology Group Criteria), 0–2; no prior thoracic irradiation; no other simultaneous malignancies; and no restrictions on previous chemotherapy. Most patients had a whole-body fluorine-18 fludeoxyglucose (¹⁸F-FDG) positron emission tomography (PET) scan. A confirmed histological diagnosis was obtained for 22 (79%) patients. The pre-treatment and follow-up CT scans and clinical records were retrospectively reviewed, with the approval obtained from our institutional review board. Written informed consent was obtained from all patients.

Treatment

All patients were positioned supine on a wing board and immobilized by means of thermoplastic frames. Two series of CT scans were acquired in the inspiratory and expiratory phases, at 3-mm slice thickness, in order to track the motion of tumours and internal organs. We defined gross tumour volume (GTV) through the superimposition of each visible tumour on two series of CT scans delineated with the lung CT window setting (window level = –550 HU, width = 1600 HU) to obtain an internal target volume (ITV). The planning target volume (PTV) was created by expanding the ITV by a uniform 5-mm margin to compensate for set-up errors and residual respiratory motion.

Overall, the median PTV was 47.31 cm³ (range, 9.4–254.5 cm³), and the median GTV was 6.43 cm³ (range, 0.65–73.70 cm³). The choice of radiation schedule was based on a risk-adapted

strategy, on target volume and type/site of lesion. The biological effective dose (BED10) was ≥ 100 Gy in 22 peripheral lesions, where the total prescribed dose was 50 Gy/5 fractions and was <100 Gy in 4 peripheral large lesions (volume, >90 cm³) and 5 centrally located lesions, which received a total prescribed dose of 50 Gy/10 fractions and 52.5 Gy/7 fractions, respectively (Table 1). The optimization was driven with the aim of delivering the prescribed dose to at least 95% of the PTV, while keeping the maximum dose (D_{\max}) to the PTV <105% of the prescribed dose with heterogeneity corrections. Specific dosimetric guidelines for organs at risk (OARs) in accordance to the QUANTEC²³ dose–volume model were applied. Dose computation and treatment delivery were performed on the TomoTherapy® Hi-Art® II System (TomoTherapy Inc., Madison, WI). Image-guided radiotherapy (RT) was performed by means of megavolt CT before each daily fraction. The delivery parameters usually adopted for treatment planning and optimization were field width, 2.5 cm; pitch, 0.287; modulation factor, 2.5; dose calculation grid, 0.215 × 0.215 cm.

Follow-up and statistics

Routine patient follow-up consisted of outpatient assessments performed 1 month post-SBRT (physical examination + chest radiography) and every 3 months in the next 2 years, alternating a quarterly diagnostic CT scan of the thorax and upper abdomen with a semi-annually total body CT scan. A post-treatment ¹⁸F-FDG/PET-CT was routinely carried out between 4 and 6 months after treatment completion and for suspected progressive disease. Toxicity monitoring was focused on treatment-related pulmonary adverse events according to the Common Terminology Criteria for Adverse Events v. 4.0:²⁴ grade 1 (asymptomatic or requiring no treatment), grade 2 [symptomatic, requiring medical intervention or limiting instrumental active daily life (ADL)], grade 3 (severely symptomatic, limiting self care and ADL, or oxygen indicated), grade 4 [life threatening, respiratory compromise, urgent intervention indicated (e.g. tracheostomy or intubation)] and grade 5 (death). Any increase in grade from baseline was considered treatment-related toxicity and graded as acute (90 days from start of RT) and late (beyond 90 days).

Patterns of lung injury were based on CT findings and considered as radiation pneumonitis (RP) or radiation fibrosis (RF), when they occurred within or later than 6 months, respectively. RP was classified into five patterns based on Ikezoe's report:²⁵ (1) diffuse consolidation, (2) patchy consolidation and ground-glass opacities (GGOs), (3) diffuse GGO, (4) patchy GGO and (5) no evidence of increased density. RF was graded according to Koenig's classification²⁶ as follows: (1) modified conventional pattern (consolidation, volume loss and bronchiectasis similar to, but less extensive than, conventional RF), (2) mass-like pattern (focal consolidation limited around the tumour), (3) scar-like pattern (linear opacity in the region of the tumour associated with volume loss).

Assessment of tumour response was based on the European Organization for Research and Treatment of Cancer Response Evaluation Criteria in Solid Tumours criteria v. 1.1,²⁷ coupled with a ¹⁸F-FDG/PET-CT scan whenever CT findings alone were

Table 1. Patient ($n = 28$), tumour ($n = 31$) and radiation treatment characteristics

| Imaging findings | Number of patients/ number of lesions (percentage of the total) |
|--|---|
| Mean age (years) | 74 |
| Range (years) | 59–88 |
| Gender | |
| Male | 22 (79) |
| Female | 6 (21) |
| Chronic obstructive pulmonary disease class | |
| GOLD 3: $30\% \leq FEV_1 < 50\%$ predicted | 21 (75) |
| GOLD 2: $50\% \leq FEV_1 < 80\%$ predicted | 7 (25) |
| Type of early stage non-small-cell lung cancer | |
| Adenocarcinoma | 15 (54) |
| Squamous cell | 7 (25) |
| Unspecified | 6 (21) |
| Maximal tumour diameter (cm) | |
| Median | 1.9 |
| Range | 0.5–3.6 |
| Planning treatment volume volume (cm^3) | |
| Median | 47.31 |
| Range | 9.4–254.5 |
| Gross tumour volume (cm^3) | |
| Median | 6.43 |
| Range | 0.65–73.7 |
| Dose prescription (per lesions) | |
| Peripheral lesions | |
| Full dose (50 Gy/5 fractions) | 22 (71) |
| Peripheral large lesions | |
| 50 Gy/10 fractions | 4 (13) |
| Central lesions | |
| 52.5 Gy/7 fractions | 5 (16) |
| Corresponding BED10 (Gy) | |
| ≥ 100 | 22 (71) |
| < 100 | 9 (29) |

BED10, biological effective dose for α/β ratio of 10; FEV₁, forced expiratory volume in the first second; GOLD, Global Initiative for Obstructive Lung Disease.

uncertain. Local failure (LF) was defined as re-growth of the disease within or at the margin of the PTV, whereas recurrence in the ipsilateral/contralateral lung or extrathoracic sites was defined as distant failure (DF).

Subgroups were compared with the log-rank test in order to find potential predictive factors. The Fisher exact test ($n < 5$) or the χ^2 test was used to determine predictive factors for lung fibrosis and clinical response. Parameters evaluated as potential predictive factors for type of response were tumour-related factors and BED. Parameters evaluated as potential predictive factors for RP or lung fibrosis were dosimetric parameters [percentage of lung volume receiving 5 Gy (V_5), percentage of lung volume receiving 10 Gy (V_{10}), mean lung dose (MLD), contralateral MLD], tumour-related factors, BED and COPD. Statistical analysis was performed using the SPSS® statistical software package v. 22 (IBM Corporation, Armonk, NY).

RESULTS

Toxicity rates and lung injury patterns

This study included 28 patients with 31 lesions treated between January 2012 and January 2014. The median follow-up time was 12 months (range, 4–20 months). 30- and 90-day mortality rates were 0%. Grade 1 acute oesophagitis was observed in two (7%) patients; one of these patients had a centrally located tumour. Overall, RP occurred 3 months after the completion of RT; one (3.5%) patient experienced a clinically severe (grade 3) pneumonitis, while grade 2 RP was observed in four (14%) patients. No correlations between the severity of RP and radiological sequelae after SBRT were found. No instances of symptomatic RF nor other treatment-related late effects (*i.e.* plexopathy, rib fractures or chest pain) were documented.

Of the 31 treated lesions, CT appearance of acute RP (6 months or less after HT-SBRT) was classified as follows: diffuse consolidation in two (6.5%) lesions; patchy consolidation and GGO in two (6.5%) lesions; diffuse GGO not observed (0%); patchy GGO in two (6.5%) lesions. Of the 25 treated lesions, CT appearance of RF (more than 6 months after HT-SBRT) was classified as follows: modified conventional pattern in three (12%) lesions, mass-like pattern in four (16%) lesions, scar-like pattern in three (12%) lesions. There was no evidence of late lung injury in 15 (60%) patients (Table 2). The calculated mean \pm standard deviation of dosimetric parameters were as follows: V_5 , $43.21 \pm 14.73\%$; V_{10} , $30.39 \pm 12.15\%$; MLD, 5.03 ± 1.92 Gy; and contralateral MLD, 2.37 ± 1.05 Gy. No statistical correlation was found between lung fibrosis and BED, COPD, dosimetric or tumour parameters.

Response and disease progression

Among the 31 treated lesions, complete response (CR) occurred in 7 (23%) cases and partial response (PR) occurred in 19 (61%) cases with a tumour response rate of 84%. After RT, five (16%) patients presented with local stable disease.

LF was observed in four (13%) patients. DF occurred in five (16%) patients (lung, two patients; brain, one patient; adrenal gland, one patient; diffuse disease, one patient).

Survival, local control and prognostic factors

At the time of the analysis, 23 patients were alive. 2 patients were alive with pulmonary disease (distant, 1 patient; local, 1 patient), while 21 patients had no evidence of disease. The median follow up of the survivors was 12 months (range, 4–20 months). The tumour

Table 2. Patterns of lung injury: early radiological findings of acute pneumonitis and late radiological findings of radiation fibrosis

| Variables | Events (%) |
|--|------------|
| ≤6 months after hypo-HT (<i>n</i> = 31) | |
| No findings | 25 (80.6) |
| Patchy GGO | 2 (6.5) |
| Diffuse GGO | – |
| Patchy consolidation and GGO | 2 (6.5) |
| Diffuse consolidation | 2 (6.5) |
| >6 months after hypo-HT (<i>n</i> = 25) | |
| No findings | 15 (60.0) |
| Modified conventional pattern | 3 (12.0) |
| Mass-like | 4 (16.0) |
| Scar-like | 3 (12.0) |

GGO, ground-glass opacity; HT, helical tomotherapy.

response rate was 84% (CR + PR). Local control was 83% at 1 year. On univariate analysis, GTV and PTV emerged as significant prognostic factors for local control ($p = 0.001$ and $p = 0.011$, respectively). Tumour-related factors such as tumour maximal diameter ($p = 0.05$), GTV ($p = 0.019$), PTV ($p = 0.001$) had significant impact on response, whereas neither patient-related nor tumour-related or dosimetric factors impacted lung fibrosis (Table 3).

DISCUSSION

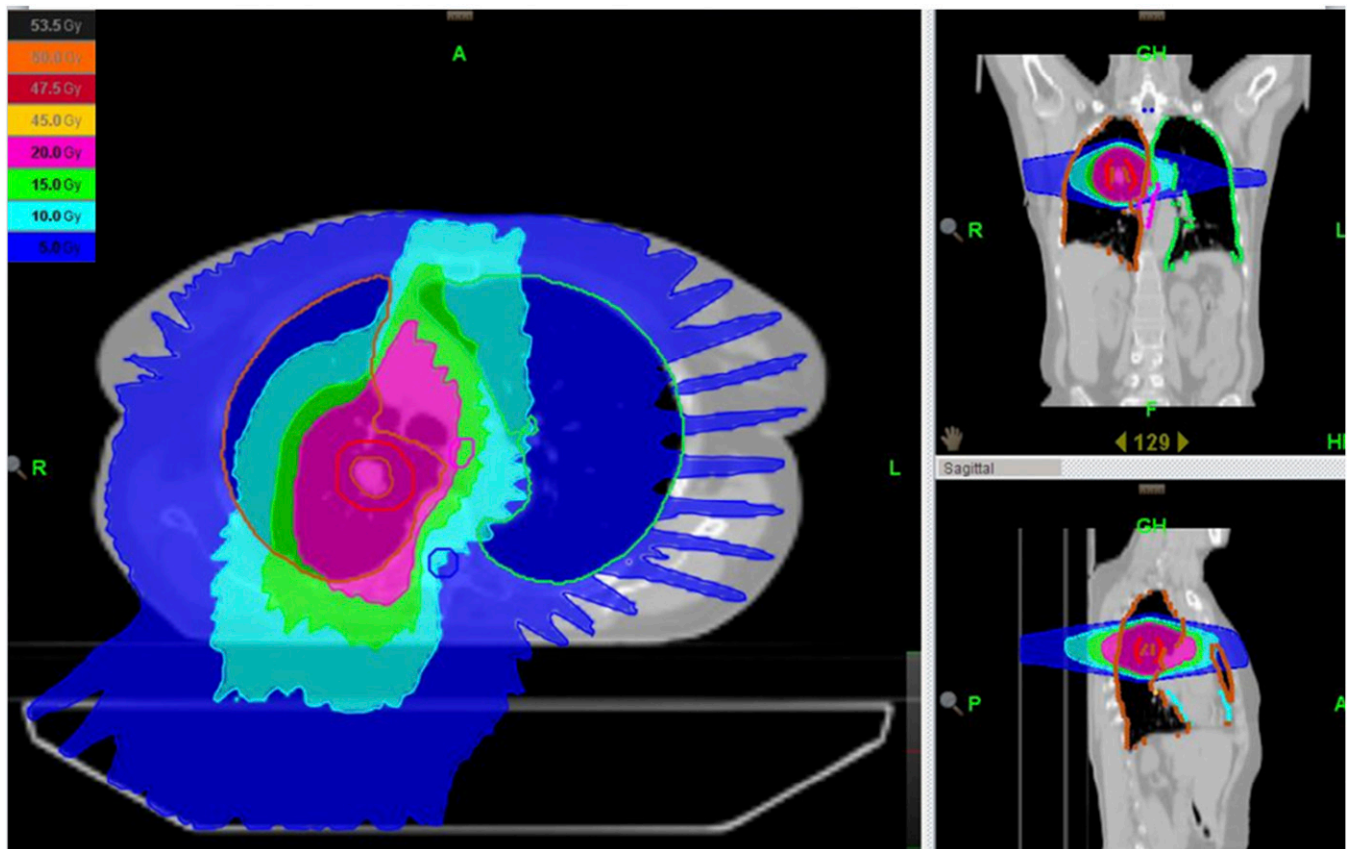
Lung lesions, either primary or metastatic, represent the paradigm of the potential benefit achievable by SBRT because the lung is deemed to be a parallel organ where the risk of radio-induced normal tissue toxicity is expected to be lower when small volumes are irradiated with large fraction sizes.²⁸ Therefore, SBRT is increasingly being considered as the preferred treatment option in patients unfit for surgery.^{9,10} A wide range of SBRT techniques are currently available for lung SBRT, including 3D-CRT, IMRT, volumetric modulated arc therapy (VMAT) and HT, and all of them could result in different patterns of radiological pneumonitis owing to differences in dose distributions. In this scenario, data on the influence of treatment techniques on rates of clinical and radiological pneumonitis are scarce. The largest study examining radiological changes and the first to compare two different treatment planning techniques (RapidArc® vs 3D-CRT) for lung SBRT comes from Palma et al²⁹ who showed that both techniques resulted in similarly low rates of clinical pneumonitis and similar severity and patterns of radiological changes. In a dosimetric study, Chi et al³⁰ compared HT-based with VMAT-based SBRT for centrally located lung lesions and found that HT appears to be superior to VMAT in OAR sparing mainly in cases that require conformal dose avoidance of multiple immediately adjacent OARs. However, HT's complex delivery of radiation dose to the target volume and to the adjacent organs over 360° of rotation with 51 projections per rotation¹² in association with the high dose per fraction can potentially result in a large distribution of low-dose radiation to the lung, typically composed of functional subunits

Table 3. Univariate analysis for lung fibrosis and complete response (CR) (p -values)

| Variables | Univariate analysis, p -value | |
|--|---------------------------------|-------|
| | Lung fibrosis | CR |
| Patient-related factors | | |
| Chronic obstructive pulmonary disease (GOLD 3 vs GOLD 2) | 0.626 | |
| Tumour-related factors | | |
| Maximal diameter (≥ 23 vs < 23 mm) | 0.511 | 0.143 |
| Maximal diameter (≥ 20 vs < 20 mm) | 0.454 | 0.050 |
| PTV (≥ 50 vs < 50 cm ³) | 0.250 | 0.004 |
| PTV (≥ 42 vs < 42 cm ³) | 0.363 | 0.001 |
| GTV (≥ 7 vs < 7 cm ³) | 0.250 | 0.004 |
| GTV (≥ 12 vs < 12 cm ³) | 0.215 | 0.019 |
| Tumour location (peripheral vs central) | 0.542 | 0.312 |
| Dosimetric parameters | | |
| V_5 (< 43 vs ≥ 43 Gy) | 0.856 | |
| V_{10} (< 30 vs ≥ 30 Gy) | 0.694 | |
| MLD (≥ 6 vs < 6 Gy) | 0.077 | |
| Controlateral MLD (≥ 3 vs < 3 Gy) | 0.068 | |
| Biological effective dose (100 vs < 100) | 0.683 | 0.484 |

GOLD, Global Initiative for Obstructive Lung Disease; GTV, gross tumour volume; MLD, mean lung dose; PTV, planning target volume; V_x , percentage of lung volume receiving x Gy.

Figure 1. A typical dose distribution of a stereotactic plan with helical tomotherapy (axial CT images with low dose regions).



arranged in a parallel architecture (Figure 1). As such, patterns of lung injury might be different than those observed with conventional 3D-CRT or other SBRT techniques (Figure 2). Understanding these changes becomes even more crucial for patients with lung lesions, whose health is compromised by factors that rule out surgical resection. While HT-SBRT is gaining traction in clinical practice, few studies—often evaluating small series of patients with inhomogeneous characteristics and short follow-up—are available in the recent literature^{15–21} (Table 4). Owing to the risk that the helical radiation delivery method, involving low-dose exposure of almost the entire contralateral lung, could also affect radiation tolerance in the high-dose regions—the so-called “bath-and-shower effect”³¹—close attention in our series has been paid to V_5 , V_{10} , MLD and contralateral MLD, which were kept well below the thresholds suggested from QUANTEC²³ in order to reduce the development of RP. In our series, the incidence of \geq grade 2 RP reached 17.5%, similar to the 5–20% rates of RP reported from several investigators for lung SBRT.^{32–36} Moreover, most of the symptomatic RP was grade 2, and only one patient experienced a grade 3 RP, less than the 6.4% incidence of grade 3 RP reported from McGarry et al³⁷ after lung SBRT in a similar patient population. When investigating the predictive factors potentially involved in the development of RP, we could not find dosimetric or clinical factors significantly associated with treatment-related toxicity. These findings seem in contrast to some recent series, employing HT either in a conventional or in a SBRT schedule for primary and metastatic lung tumours,

where cut-off values for ipsilateral³⁸ and contralateral V_5 ^{17,39} have been proposed, and GTV was found as the only predictive factor significantly associated with grade 5 RP.²⁰ Guckenberger et al⁴⁰ reported the association of low-dose radiation distribution with the development of RP after SBRT, with an incidence of RP of 18.6%. Some authors provided detailed radiological descriptions of lung appearances after SBRT; Huang et al⁴¹ in

Figure 2. A case of diffuse consolidation pattern of a radiological pneumonitis 3 months after stereotactic body radiotherapy delivered with helical tomotherapy.

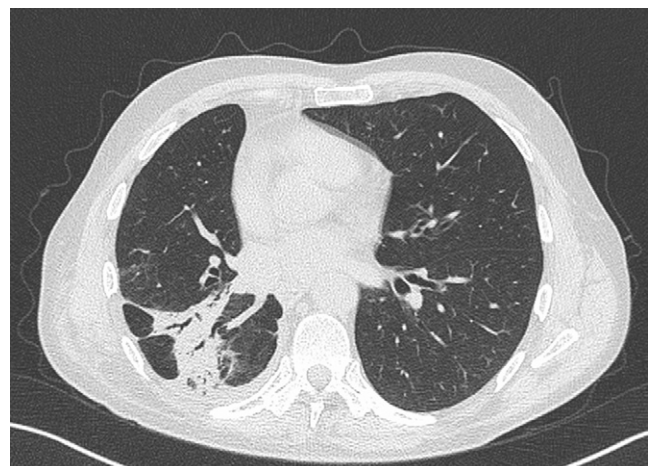


Table 4. Studies of stereotactic radiotherapy for lung tumours treated with helical tomotherapy

| Study | Number of patients | Number of lesions | Radiation therapy regimen | Median follow-up (months) | Local control | Overall survival | Severe toxicity grade ≥ 3 (%) |
|-------------------------------|--------------------|-------------------|---------------------------|---------------------------|------------------------------|------------------------------|------------------------------------|
| Hodge et al ¹⁵ | 9 (NSCLC) | 9 | 60 Gy/5 fractions | 12 | NR | NR | 0 |
| Kim et al ¹⁶ | 31 (Mts) | 31 | 40–50 Gy/10 fractions | 13 | 1 year, 87.1% | 1 year, 60.5% | 0 |
| Sole et al ¹⁸ | 42 (Mts) | 60 | 60 Gy/3–8 fractions | 15 | 1 year, 92%; 2 years, 86% | 1 year, 84%; 2 years, 63% | 5 |
| Marcenaro et al ¹⁹ | 74 (NSCLC/Mts) | 74 | 48–60 Gy/4–8 fractions | 15 | 2 years, 55.4% | 2 years, 58% | 0 |
| Aibe et al ²⁰ | 30 (NSCLC) | 31 | 50 Gy/5 fractions | 36.5 | 1 year, 93%; 2 years, 73% | 1 year, 83%; 2 years, 77% | 7 |
| Rosen et al ²¹ | 79 (NSCLC) | 79 | 48–60 Gy/4–5 fractions | 27 | 1 year, 93.6% | 1 year, 92.3% | NR |

Mts, metastases; NR, not reported; NSCLC, non-small-cell lung cancer.

a systematic review observed that acute changes post-SBRT predominantly appear as consolidation or GGOs, while late changes often demonstrate a modified conventional pattern of fibrosis. Trovo et al⁴² found that patients who developed more than grade 2 pneumonitis after SBRT showed patchy consolidation and GGO, and patchy GGO more frequently than other patterns. In our series, we were not able to observe a preferential pattern either in the acute or late setting, nor a correlation between acute and late changes over time. Interestingly, not even a correlation between radiological appearance, the delivered dose and the tumour volume was found, in agreement with a larger series of 68 patients (70 tumours), whose radiological changes after SBRT were investigated and correlated with treatment characteristics.⁴³ The aforementioned differences between our observations and some findings in the existing literature may be owing to several factors such as patient characteristics, sample size, SBRT treatment technique, follow-up duration and interobserver variations. One of the main limitations of our study is certainly related to the relatively short follow-up that cannot exclude that structural changes may theoretically occur later, being the fibrotic evolution after high-dose irradiation a dynamic process that might continue for many years.^{44–46} Nevertheless, when analysing the temporal pattern of CT changes after SBRT, Dahele et al⁴⁷ found that the

actuarial median time to first CT changes was 17 weeks, whereas Hof et al⁴⁸ showed that CT changes increase with dose and peak at 16 weeks after single-fraction lung radiosurgery. Therefore, the median follow-up of 12 months in our cohort almost entirely covered the time course of treatment-related toxicity as well as patterns of radiological lung injury. A further limitation of our experience is that the scoring of CT changes after lung SBRT herein adopted^{25,26} is qualitative and may be subjective. Alternative methods, such as the use of CT density changes, may represent an objective measure of lung damage because density changes strongly correlate with histological findings of inflammation,⁴⁹ thus allowing for a more robust dose–response relationship based on quantitative data.^{50,51}

CONCLUSION

Notwithstanding the retrospective nature and its intrinsic inherent biases, our study shows that HT-SBRT can be considered an effective treatment with a mild toxicity profile in a medically inoperable patient population with early stage NSCLC, provided that careful attention is paid to low-dose exposure of normal lung. Although a specific pattern of lung injury was not found to be associated with this technique, patients should be carefully followed, and long-term results are warranted.

REFERENCES

- Chang MY, Sugarbaker DJ. Surgery for early stage non-small cell lung cancer. *Semin Surg Oncol* 2003; **21**: 74–84.
- Edwards BK, Howe HL, Ries LA, Thun MJ, Rosenberg HM, Yancik R, et al. Annual report to the nation on the status of cancer, 1973–1999, featuring implications of age and aging on US cancer burden. *Cancer* 2002; **94**: 2766–92.
- Audisio RA, Zbar AP, Jaklitsch MT. Surgical management of oncogeriatric patients. *J Clin Oncol* 2007; **25**: 1924–9.
- Chi A, Liao Z, Nguyen NP, Xu J, Stea B, Komaki R. Systemic review of the patterns of failure following stereotactic body radiation therapy in early-stage non-small-cell lung cancer: clinical implications. *Radiother Oncol* 2010; **94**: 1–11. doi: [10.1016/j.radonc.2009.12.008](https://doi.org/10.1016/j.radonc.2009.12.008)

5. Chang JY, Balter PA, Dong L, Yang Q, Liao Z, Jeter M, et al. Stereotactic body radiation therapy in centrally and superiorly located stage I or isolated recurrent non-small-cell lung cancer. *Int J Radiat Oncol Biol Phys* 2008; **72**: 967–71. doi: [10.1016/j.ijrobp.2008.08.001](https://doi.org/10.1016/j.ijrobp.2008.08.001)
6. Osti MF, Carnevale A, Valeriani M, De Sanctis V, Minniti G, Cortesi E, et al. Clinical outcomes of single dose stereotactic radiotherapy for lung metastases. *Clin Lung Cancer* 2013; **14**: 699–703. doi: [10.1016/j.clcc.2013.06.006](https://doi.org/10.1016/j.clcc.2013.06.006)
7. Ricardi U, Frezza G, Filippi AR, Badellino S, Levis M, Navarra P, et al. Stereotactic ablative radiotherapy for stage I histologically proven non-small cell lung cancer: an Italian multicenter observational study. *Lung Cancer* 2014; **84**: 248–53. doi: [10.1016/j.lungcan.2014.02.015](https://doi.org/10.1016/j.lungcan.2014.02.015)
8. Filippi AR, Badellino S, Guarneri A, Levis M, Botticella A, Mantovani C, et al. Outcomes of single fraction stereotactic ablative radiotherapy for lung metastases. *Technol Cancer Res Treat* 2014; **13**: 37–45. doi: [10.7785/ctrt.2012.500355](https://doi.org/10.7785/ctrt.2012.500355)
9. Palma D, Visser O, Lagerwaard FJ, Belderbos J, Slotman BJ, Senan S, et al. Impact of introducing stereotactic lung radiotherapy for elderly patients with stage I non-small-cell lung cancer: a population-based time-trend analysis. *J Clin Oncol* 2010; **28**: 5153–9. doi: [10.1200/JCO.2010.30.0731](https://doi.org/10.1200/JCO.2010.30.0731)
10. Palma DA, Senan S. Improving outcomes for high-risk patients with early-stage non-small-cell lung cancer: insights from population-based data and the role of stereotactic ablative radiotherapy. *Clin Lung Cancer* 2013; **14**: 1–5. doi: [10.1016/j.clcc.2012.06.005](https://doi.org/10.1016/j.clcc.2012.06.005)
11. Kupelian P, Langen K. Helical tomotherapy: image-guided and adaptive radiotherapy. *Front Radiat Ther Oncol* 2011; **43**: 165–80. doi: [10.1159/000322420](https://doi.org/10.1159/000322420)
12. Mackie TR, Balog J, Ruchala K, Shepard D, Aldridge S, Fitchard E, et al. Tomotherapy. *Semin Radiat Oncol* 1999; **9**: 108–17.
13. Shi C, Peñagaricano J, Papanikolaou N. Comparison of IMRT treatment plans between linac and helical tomotherapy based on integral dose and inhomogeneity index. *Med Dosim* 2008; **33**: 215–21. doi: [10.1016/j.meddos.2007.11.001](https://doi.org/10.1016/j.meddos.2007.11.001)
14. Lee TF, Fang FM, Chao PJ, Su TJ, Wang LK, Leung SW. Dosimetric comparison of helical tomotherapy and step-and-shoot intensity modulated radiotherapy in nasopharyngeal carcinoma. *Radiation Oncol* 2008; **89**: 89–96. doi: [10.1016/j.radonc.2008.05.010](https://doi.org/10.1016/j.radonc.2008.05.010)
15. Hodge W, Tomé WA, Jaradat HA, Orton NP, Khuntia D, Traynor A, et al. Feasibility report of image guided stereotactic body radiotherapy (IG-SBRT) with tomotherapy for early stage medically inoperable lung cancer using extreme hypofractionation. *Acta Oncol* 2006; **45**: 890–6.
16. Kim JY, Kay CS, Kim YS, Jang JW, Bae SH, Choi JY, et al. Helical tomotherapy for simultaneous multitarget radiotherapy for pulmonary metastasis. *Int J Radiat Oncol Biol Phys* 2009; **75**: 703–10. doi: [10.1016/j.ijrobp.2008.11.065](https://doi.org/10.1016/j.ijrobp.2008.11.065)
17. Kim Y, Hong SE, Kong M, Choi J. Predictive factors for radiation pneumonitis in lung cancer treated with helical tomotherapy. *Cancer Res Treat* 2013; **45**: 295–302. doi: [10.4143/crt.2013.45.4.295](https://doi.org/10.4143/crt.2013.45.4.295)
18. Sole CV, Lopez Guerra JL, Matute R, Jaen J, Puebla F, Rivin E, et al. Stereotactic ablative radiotherapy delivered by image-guided helical tomotherapy for extracranial oligometastases. *Clin Transl Oncol* 2013; **15**: 484–91. doi: [10.1007/s12094-012-0956-2](https://doi.org/10.1007/s12094-012-0956-2)
19. Marcenaro M, Vagge S, Belgioia L, Agnese D, Lamanna G, Mantero E, et al. Ablative or palliative stereotactic body radiotherapy with helical tomotherapy for primary or metastatic lung tumor. *Anticancer Res* 2013; **33**: 655–60.
20. Aibe N, Yamazaki H, Nakamura S, Tsubokura T, Kobayashi K, Kodani N, et al. Outcome and toxicity of stereotactic body radiotherapy with helical tomotherapy for inoperable lung tumor: analysis of grade 5 radiation pneumonitis. *J Radiat Res* 2014; **55**: 575–82. doi: [10.1093/jrr/rrt146](https://doi.org/10.1093/jrr/rrt146)
21. Rosen LR, Fischer-Valuck BW, Katz SR, Durci M, Wu HT, Syh J, et al. Helical image-guided stereotactic body radiotherapy (SBRT) for the treatment of early-stage lung cancer: a single institution experience at the Willis-Knighton Cancer Center. *Tumori* 2014; **100**: 42–8. doi: [10.1700/1430.15814](https://doi.org/10.1700/1430.15814)
22. Rabe KF, Hurd S, Anzueto A, Barnes PJ, Buist SA, Calverley P, et al; Global Initiative for Chronic Obstructive Lung Disease. Global strategy for the diagnosis, management, and prevention of chronic obstructive pulmonary disease: GOLD executive summary. *Am J Respir Crit Care Med* 2007; **176**: 532–55.
23. Jackson A, Marks LB, Bentzen SM, Eisbruch A, Yorke ED, Ten Haken RK, et al. The lessons of QUANTEC: recommendations for reporting and gathering data on dose-volume dependencies of treatment outcome. *Int J Radiat Oncol Biol Phys* 2010; **76**: S155–60. doi: [10.1016/j.ijrobp.2009.08.074](https://doi.org/10.1016/j.ijrobp.2009.08.074)
24. National Cancer Institute. Common terminology criteria for adverse events v.4.0. Available from: http://evs.nci.nih.gov/ftp1/CTCAE/CTCAE_4.03_2010-06-14_QuickReference_5x7.pdf
25. Ikezoe J, Takashima S, Morimoto S, Kadowaki K, Takeuchi N, Yamamoto T, et al. CT appearance of acute radiation-induced injury in the lung. *AJR Am J Roentgenol* 1988; **150**: 765–70.
26. Koenig TR, Munden RF, Erasmus JJ, Sabloff BS, Gladish GW, Komaki R, et al. Radiation injury of the lung after three-dimensional conformal radiation therapy. *AJR Am J Roentgenol* 2002; **178**: 1383–8.
27. Eisenhauer EA, Therasse P, Bogaerts J, Schwartz LH, Sargent D, Ford R, et al. New response evaluation criteria in solid tumors: revised RECIST guideline (version 1.1). *Eur J Cancer* 2009; **45**: 228–47. doi: [10.1016/j.ejca.2008.10.026](https://doi.org/10.1016/j.ejca.2008.10.026)
28. Emami B, Lyman J, Brown A, Coia L, Goitein M, Munzenrider JE, et al. Tolerance of normal tissue to therapeutic irradiation. *Int J Radiat Oncol Biol Phys* 1991; **21**: 109–22.
29. Palma DA, Senan S, Haasbeek CJ, Verbakel WF, Vincent A, Lagerwaard F. Radiological and clinical pneumonitis after stereotactic lung radiotherapy: a matched analysis of three-dimensional conformal and volumetric-modulated arc therapy techniques. *Int J Radiat Oncol Biol Phys* 2011; **80**: 506–13. doi: [10.1016/j.ijrobp.2010.02.032](https://doi.org/10.1016/j.ijrobp.2010.02.032)
30. Chi A, Ma P, Fu G, Hobbs G, Welsh JS, Nguyen NP, et al. Critical structure sparing in stereotactic ablative radiotherapy for central lung lesions: helical tomotherapy vs. volumetric modulated arc therapy. *PLoS One* 2013; **8**: e59729. doi: [10.1371/journal.pone.0059729](https://doi.org/10.1371/journal.pone.0059729)
31. van Luijk P, Faber H, Schippers JM, Brandenburg S, Langendijk JA, Meertens H, et al. Bath and shower effects in the rat parotid gland explain increased relative risk of parotid gland dysfunction after intensity-modulated radiotherapy. *Int J Radiat Oncol Biol Phys* 2009; **74**: 1002–5. doi: [10.1016/j.ijrobp.2009.03.039](https://doi.org/10.1016/j.ijrobp.2009.03.039)
32. Takeda A, Sanuki N, Kunieda E, Ohashi T, Oku Y, Takeda T, et al. Stereotactic body radiotherapy for primary lung cancer at a dose of 50 Gy total in five fractions to the periphery of the planning target volume calculated using a superposition algorithm. *Int J Radiat Oncol Biol Phys* 2009; **73**: 442–8. doi: [10.1016/j.ijrobp.2008.04.043](https://doi.org/10.1016/j.ijrobp.2008.04.043)
33. Matsuo Y, Shibuya K, Nakamura M, Narabayashi M, Sakanaka K, Ueki N, et al. Dose-volume metrics associated with radiation pneumonitis after stereotactic body radiation therapy for lung cancer. *Int J Radiat Oncol Biol Phys* 2012; **83**: e545–9. doi: [10.1016/j.ijrobp.2012.01.018](https://doi.org/10.1016/j.ijrobp.2012.01.018)
34. Inoue T, Katoh N, Onimaru R, Shimizu S, Tsuchiya K, Suzuki R, et al. Stereotactic body radiotherapy using gated radiotherapy with real-time tumor-tracking for stage I non-small cell lung cancer. *Radiat Oncol* 2013; **8**: 69. doi: [10.1186/1748-717X-8-69](https://doi.org/10.1186/1748-717X-8-69)

35. Baker R, Han G, Sarangkasiri S, DeMarco M, Turke C, Stevens CW, et al. Clinical and dosimetric predictors of radiation pneumonitis in a large series of patients treated with stereotactic body radiation therapy to the lung. *Int J Radiat Oncol Biol Phys* 2013; **85**: 190–5. doi: [10.1016/j.ijrobp.2012.03.041](https://doi.org/10.1016/j.ijrobp.2012.03.041)
36. Barriger RB, Forquer JA, Brabham JG, Andolino DL, Shapiro RH, Henderson MA, et al. A dose-volume analysis of radiation pneumonitis in non-small cell lung cancer patients treated with stereotactic body radiation therapy. *Int J Radiat Oncol Biol Phys* 2012; **82**: 457–62. doi: [10.1016/j.ijrobp.2010.08.056](https://doi.org/10.1016/j.ijrobp.2010.08.056)
37. McGarry RC, Papiez L, Williams M, Whitford T, Timmerman RD. Stereotactic body radiation therapy of early-stage non-small-cell lung carcinoma: phase I study. *Int J Radiat Oncol Biol Phys* 2005; **63**: 1010–15.
38. Jo IY, Kay CS, Kim JY, Son SH, Kang YN, Jung JY, et al. Significance of low-dose radiation distribution in development of radiation pneumonitis after helical-tomotherapy-based hypofractionated radiotherapy for pulmonary metastases. *J Radiat Res* 2014; **55**: 105–12. doi: [10.1093/jrr/rrt080](https://doi.org/10.1093/jrr/rrt080)
39. Song CH, Pyo H, Moon SH, Kim TH, Kim DW, Cho KH. Treatment-related pneumonitis and acute esophagitis in non-small-cell lung cancer patients treated with chemotherapy and helical tomotherapy. *Int J Radiat Oncol Biol Phys* 2010; **78**: 651–8. doi: [10.1016/j.ijrobp.2009.08.068](https://doi.org/10.1016/j.ijrobp.2009.08.068)
40. Guckenberger M, Baier K, Polat B, Richter A, Krieger T, Wilbert J, et al. Dose-response relationship for radiation-induced pneumonitis after pulmonary stereotactic body radiotherapy. *Radiother Oncol* 2010; **97**: 65–70. doi: [10.1016/j.radonc.2010.04.027](https://doi.org/10.1016/j.radonc.2010.04.027)
41. Huang K, Dahele M, Senan S, Guckenberger M, Rodrigues GB, Ward A, et al. Radiographic changes after lung stereotactic ablative radiotherapy (SABR)—can we distinguish recurrence from fibrosis? A systematic review of the literature. *Radiother Oncol* 2012; **102**: 335–42. doi: [10.1016/j.radonc.2011.12.018](https://doi.org/10.1016/j.radonc.2011.12.018)
42. Trovo M, Linda A, El Naqa I, Javidan-Nejad C, Bradley J. Early and late lung radiographic injury following stereotactic body radiation therapy (SBRT). *Lung Cancer* 2010; **69**: 77–85. doi: [10.1016/j.jungcan.2009.09.006](https://doi.org/10.1016/j.jungcan.2009.09.006)
43. Kimura T, Matsuura K, Murakami Y, Hashimoto Y, Kenjo M, Kaneyasu Y, et al. CT appearance of radiation injury of the lung and clinical symptoms after stereotactic body radiation therapy (SBRT) for lung cancers: are patients with pulmonary emphysema also candidates for SBRT for lung cancers? *Int J Radiat Oncol Biol Phys* 2006; **66**: 483–91.
44. Takeda T, Takeda A, Kunieda E, Ishizaka A, Takemasa K, Shimada K, et al. Radiation injury after hypofractionated stereotactic radiotherapy for peripheral small lung tumors: serial changes on CT. *AJR Am J Roentgenol* 2004; **182**: 1123–8.
45. Guckenberger M, Heilman K, Wulf J, Mueller G, Beckmann G, Flentje M. Pulmonary injury and tumor response after stereotactic body radiotherapy (SBRT): results of a serial follow-up CT study. *Radiother Oncol* 2007; **85**: 435–42. Erratum in: *Radiother Oncol* 2008; **86**: 293.
46. Matsuo Y, Nagata Y, Mizowaki T, Takayama K, Sakamoto T, Sakamoto M, et al. Evaluation of mass-like consolidation after stereotactic body radiation therapy for lung tumors. *Int J Clin Oncol* 2007; **12**: 356–62.
47. Dahele M, Palma D, Lagerwaard F, Slotman B, Senan S. Radiological changes after stereotactic radiotherapy for stage I lung cancer. *J Thorac Oncol* 2011; **6**: 1221–8. doi: [10.1097/JTO.0b013e318219aac5](https://doi.org/10.1097/JTO.0b013e318219aac5)
48. Hof H, Zgoda J, Nill S, Hoess A, Kopp-Schneider A, Herfarth K, et al. Time- and dose-dependency of radiographic normal tissue changes of the lung after stereotactic radiotherapy. *Int J Radiat Oncol Biol Phys* 2010; **77**: 1369–74. doi: [10.1016/j.ijrobp.2009.06.082](https://doi.org/10.1016/j.ijrobp.2009.06.082)
49. Ghobadi G, Hogeweg LE, Faber H, Tukker WG, Schippers JM, Brandenburg S, et al. Quantifying local radiation-induced lung damage from computed tomography. *Int J Radiat Oncol Biol Phys* 2010; **76**: 548–56. doi: [10.1016/j.ijrobp.2009.08.058](https://doi.org/10.1016/j.ijrobp.2009.08.058)
50. Palma DA, van Sörnsen de Koste J, Verbakel WF, Vincent A, Senan S. Lung density changes after stereotactic radiotherapy: a quantitative analysis in 50 patients. *Int J Radiat Oncol Biol Phys* 2011; **81**: 974–8. doi: [10.1016/j.ijrobp.2010.07.025](https://doi.org/10.1016/j.ijrobp.2010.07.025)
51. Mattonen SA, Palma DA, Haasbeek CJ, Senan S, Ward AD. Distinguishing radiation fibrosis from tumour recurrence after stereotactic ablative radiotherapy (SABR) for lung cancer: a quantitative analysis of CT density changes. *Acta Oncol* 2013; **52**: 910–18. doi: [10.3109/0284186X.2012.731525](https://doi.org/10.3109/0284186X.2012.731525)